Supporting Information for

Effect of the metal–support interaction on the activity and selectivity of methanol oxidation over Au supported on mesoporous oxides

***Sunyoung Oh,[1ac] You Kyung Kim,[1bc] Chan Ho Jung,[c] Won Hui Doh,[c] and Jeong Young Park**[*abc]*

[a] *Department of Chemistry, Korea Advanced Institute of Science and Technology (KAIST), Daejeon 34141, Republic of Korea.*

[b] *Graduate School of EEWS, Korea Advanced Institute of Science and Technology (KAIST), Daejeon 34141, Republic of Korea.*

[c] *Center for Nanomaterials and Chemical Reactions, Institute for Basic Science (IBS), Daejeon 34141, Republic of Korea.*

*To whom correspondence should be addressed. E-mail: jeongypark@kaist.ac.kr

Experimental Information

Synthesis

Synthesis of KIT-6 hard template. KIT-6 mesoporous silica was used as a hard template with an ordered bicontinuous mesostructure with cubic *Ia3d* symmetry.[1] To prepare the KIT-6, 17.5 g of P123 and 75 g of 35 wt% HCl were poured into a polypropylene bottle with 625.0 g of H_2O, and stirred at 35 °C to dissolve the P123. 22.4 g of n-butanol was added to the solution with subsequent stirring for 1 h. After that, 55.5 g of tetraethyl orthosilicate (TEOS) was added and the solution was aged in an oven at 35 °C for 24 h. In this step, the pore size and structure can be controlled by temperature and time. After 24 h, the solution was collected, washed with deionized (DI) water, and dried overnight in an oven at 65 °C. The white powders were mixed with HCl and ethanol, washed several times and dried again at 65 °C. The powders were then calcined in air at 550 °C for 5 h.

Synthesis of Co_3O_4, NiO, and Fe_2O_3 mesoporous oxides. Mesoporous Co_3O_4, NiO, and Fe_2O_3 oxides were synthesized using the nanocasting method, which used KIT-6 as the hard template and metal nitrate as the precursor.[2] $Co(NO_3)_2{\cdot}6H_2O$, $Ni(NO_3)_2{\cdot}6H_2O$, and $Fe(NO_3)_3{\cdot}9H_2O$ (Sigma-Aldrich) were used as precursors. 4 g of KIT-6 and 50 mL of toluene were added to 16 mmol of a metal precursor with 8 mL of DI water and stirred at 65 °C. After toluene evaporation, the precipitated solid was dried for 24 h and calcined at 300 °C for 6 h. To remove the silica template, 2 M of NaOH was added, heated at 60 °C, and washed with DI water several times.[3-5]

Au deposition on Co_3O_4, NiO, and Fe_2O_3 mesoporous oxides (Au/m-oxide). The mesoporous oxides (0.5 g) were dispersed into the 4.2 x 10^{-3} M $HAuCl_4$ solution, derived from the urea reduction method, and stirred at 80 °C. 0.42 M urea ($CO(NH_2)_2$) was added dropwise to the solution to reduce the metal precursor and attach the Au nanoparticles onto the support oxide.[6] All the procedures occurred in the absence of light because several studies have reported that Au precursors and Au nanoparticles can be decomposed by light.[7] After stirring, the solutions were washed several times with ethanol and dried in an oven at 100 °C.

Catalytic oxidation performance of methanol.

Methanol oxidation reaction. Methanol oxidation was performed in a flow reactor. Prepared samples (40 mg) were pelletized and loaded into a quartz tube. Pre-treatment was done at 250 °C for 40 min with H_2 flow (5% H_2 balanced with carrier gas He). The reactant mixture was composed of 10% gas-phase methanol and 10% O_2, balanced with He. The total flow rate was set to 50 mL min^{-1}, controlled by a mass flow controller (BROOKS instrument). The reaction was performed from 80 to 300 °C and the temperature was increased at 10 °C/17.5 min while continuously monitoring the reactant and product concentrations. The methanol oxidation reaction continued until the methanol was completely converted to carbon dioxide. Methyl formate was produced as a partial oxidation product and CO_2 was produced as the full oxidation product. The gas mixtures produced by the oxidative reaction of methanol were analyzed using gas chromatography (GC; DS Science) with a thermal conductivity detector (TCD) and flame ionization detector (FID).

	Au diameter (nm)	Au composition (wt%)	BET surface area (m^2/g)	Mean pore diameter (nm)
Au/SiO_2 (KIT-6)	5.1 ± 1.3	2.5	413.99	4.22
Au/m-Co_3O_4	5.6 ± 1.3	3.6	172.16	16.67
Au/m-NiO	5.2 ± 0.3	2	156.84	16.25
Au/m-Fe_2O_3	5.0 ± 0.8	2.7	216.91	6.60

Table S1. Results from inductively coupled plasma atomic emission spectroscopy (ICP-AES), Brunauer–Emmett–Teller (BET), and diameters of the Au supported on mesoporous oxides.

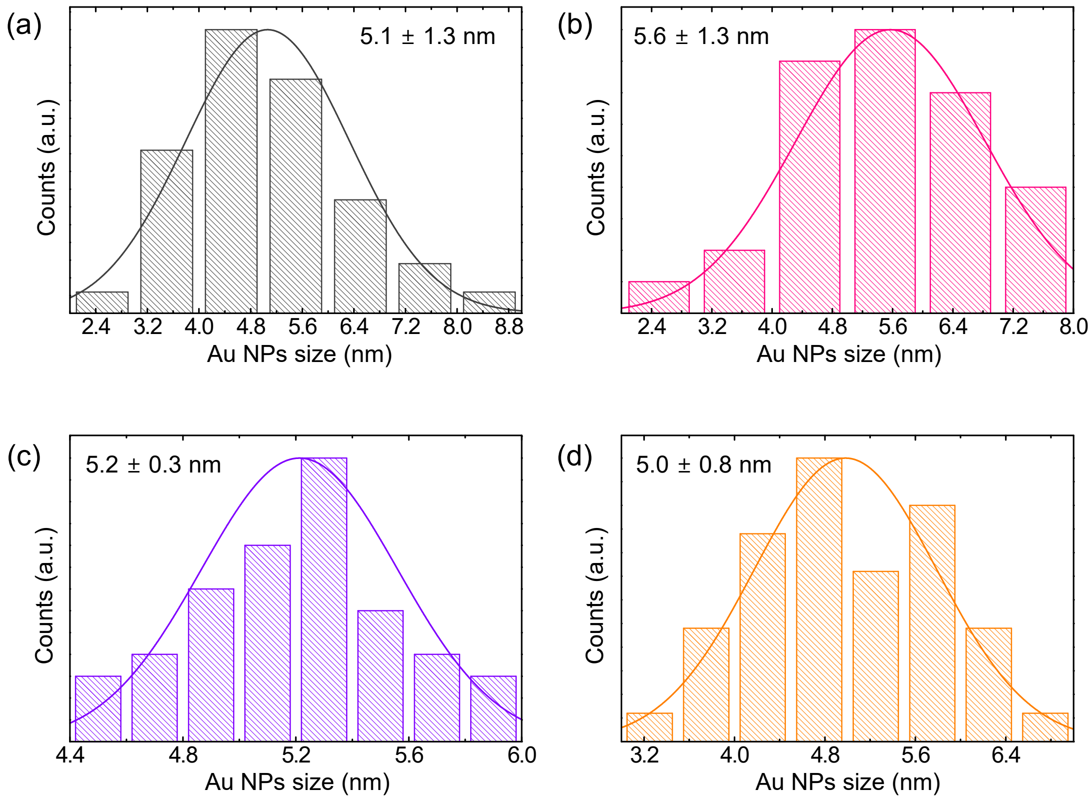

Fig. S1. Size distribution histograms of the Au nanoparticles of (a) Au/KIT-6, (b) Au/m-Co_3O_4, (c) Au/m-NiO, and (d) Au/m-Fe_2O_3.

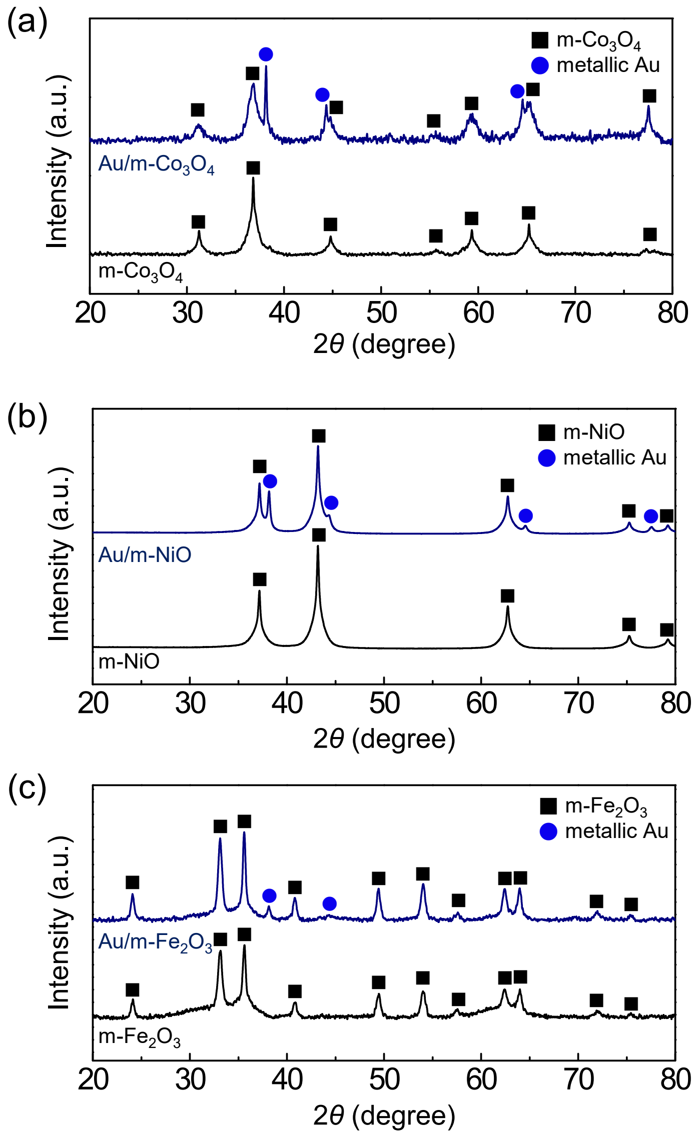

Fig. S2. XRD patterns of (a) m-Co_3O_4, (b) m-NiO, and (c) m-Fe_2O_3 with and without Au nanoparticles.[8-11]

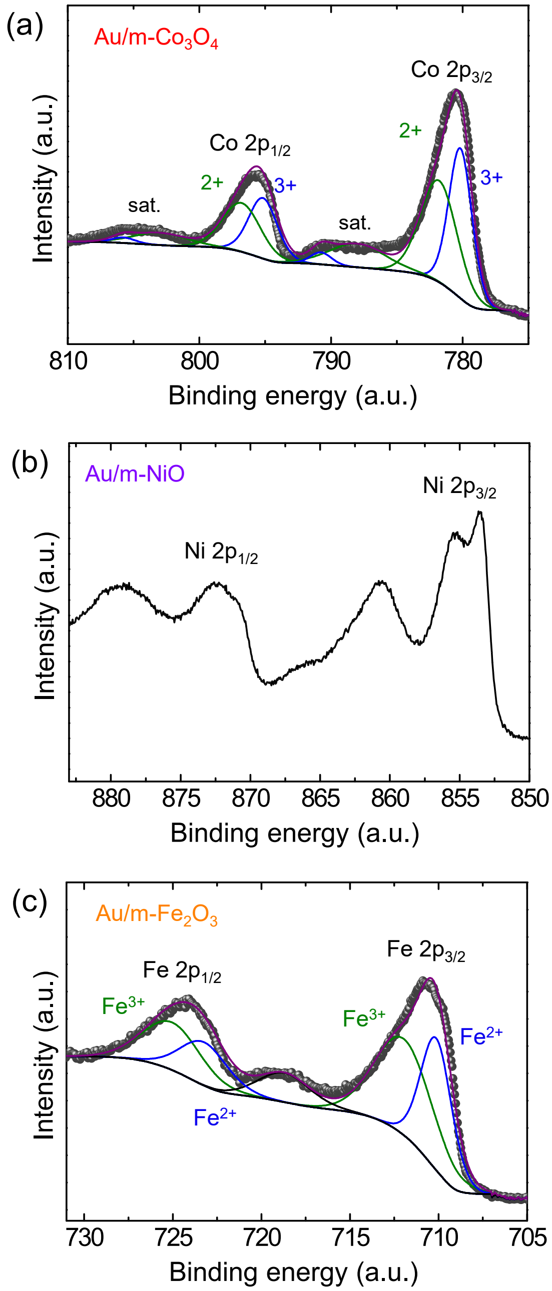

Fig. S3. XPS spectra of the Au nanoparticles supported on mesoporous oxides: (a) Co 2p of Au/m-Co_3O_4, (b) Ni 2p of Au/m-NiO, and (c) Fe 2p of Au/m-Fe_2O_3.

The Co 2p spectrum shows two main Co $2p_{3/2}$ and Co $2p_{1/2}$ peaks at 780.4 and 795.4 eV, respectively, indicating the chemical bonding states of Co_3O_4.[12] The Ni 2p spectrum shows the main peaks of NiO.[13] The XPS spectrum of Fe 2p indicates three main peaks containing Fe $2p_{3/2}$ at 710.7 eV, Fe $2p_{1/2}$ at 724.2 eV, and a satellite at 718.9 eV, which is in agreement with α-Fe_2O_3.[14]

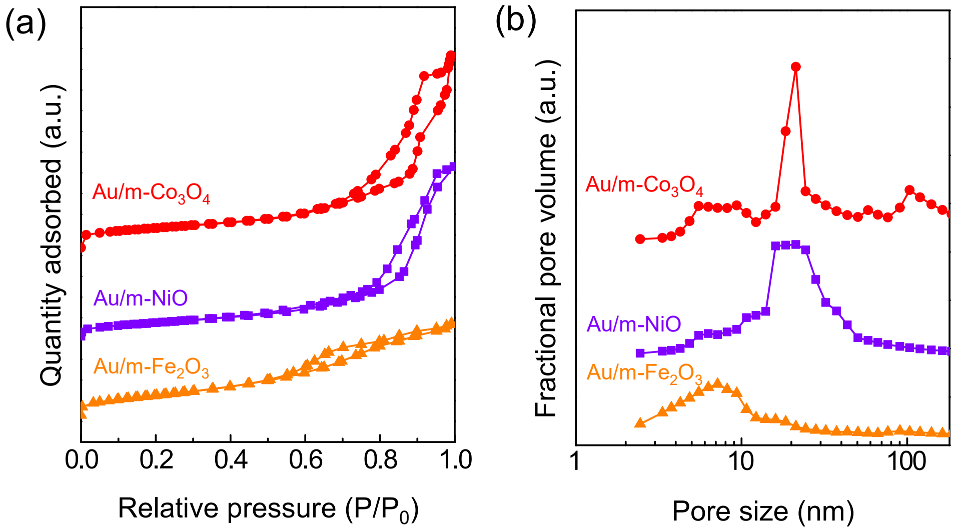

Fig. S4. (a) Nitrogen adsorption–desorption isotherms and (b) pore size distribution curves for Au/m-Co_3O_4, Au/m-NiO, and Au/m-Fe_2O_3.

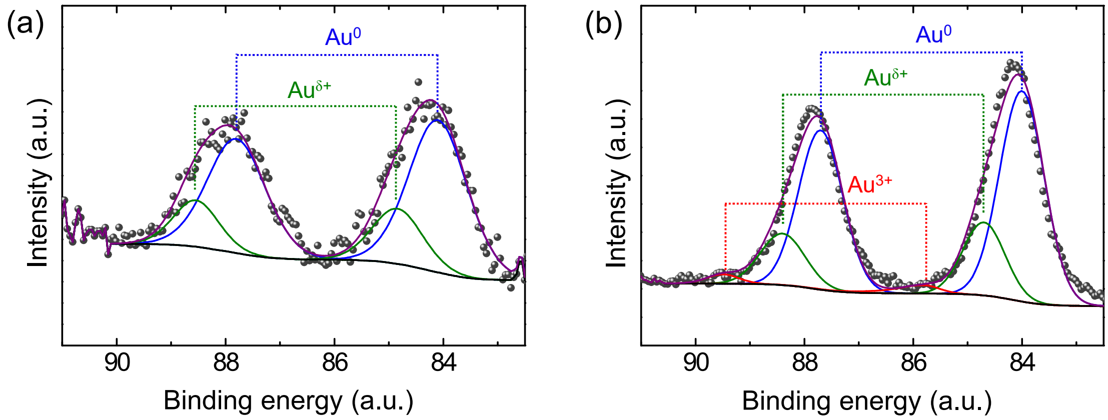

Fig. S5. XPS spectra of Au 4f for Au/m-Fe_2O_3 (a) before and (b) after the methanol oxidation reaction.

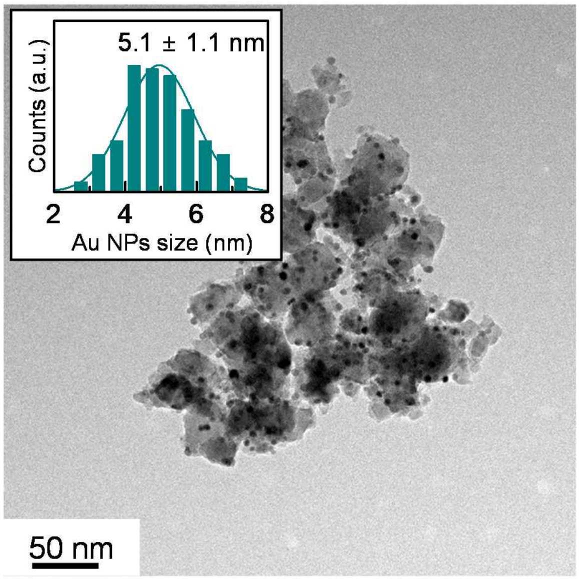

Fig. S6. Transmission electron microscopy (TEM) image and size distribution of the Au nanoparticles for the Au/m-Fe_2O_3 after methanol oxidation.

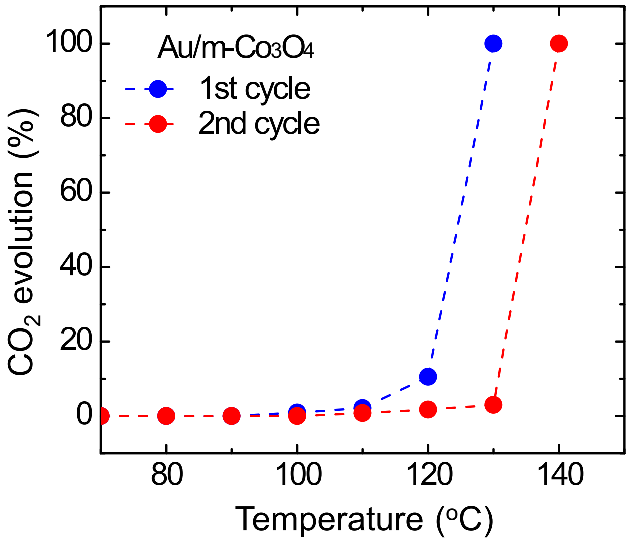

Fig. S7. Catalytic performance of repeated full-oxidation of methanol to CO_2 as a function of temperature for Au/m-Co_3O_4.

References

1. F. Kleitz, S. Hei Choi and R. Ryoo, *Chem. Comm.*, 2003, DOI: 10.1039/b306504a, 2136-2137.
2. A. H. Lu and F. Schüth, *Adv. Mater.*, 2006, **18**, 1793-1805.
3. K. An, S. Alayoglu, N. Musselwhite, S. Plamthottam, G. Melaet, A. E. Lindeman and G. A. Somorjai, *J Am Chem Soc*, 2013, **135**, 16689-16696.
4. Y. Ren, Z. Ma, L. Qian, S. Dai, H. He and P. G. Bruce, *Catal. Lett.*, 2009, **131**, 146-154.
5. A. Taguchi and F. Schüth, *Microporous Mesoporous Mater.*, 2005, **77**, 1-45.
6. R. Zanella, S. Giorgio, C. R. Henry and C. Louis, *J. Phys. Chem. B.*, 2002, **106**, 7634-7642.
7. R. Zanella, S. Giorgio, C.-H. Shin, C. R. Henry and C. Louis, *J. Catal.*, 2004, **222**, 357-367.
8. P. Dutta, M. Seehra, S. Thota and J. Kumar, *J. Phys.: Condens. Matter* 2007, **20**, 015218.
9. Z. Lockman, X. Qi, A. Berenov, R. Nast, W. Goldacker and J. MacManus-Driscoll, *Physica C: Superconductivity*, 2001, **351**, 34-37.
10. K. Woo, H. J. Lee, J. P. Ahn and Y. S. Park, *Adv. Mater.*, 2003, **15**, 1761-1764.
11. Y. Chen, X. Gu, C. G. Nie, Z. Y. Jiang, Z. X. Xie and C. J. Lin, *Chem. Comm.*, 2005, DOI: 10.1039/b504911c, 4181-4183.
12. X. Li, Y. Fang, X. Lin, M. Tian, X. An, Y. Fu, R. Li, J. Jin and J. Ma, *J. Mater. Chem.*, 2015, **3**, 17392-17402.
13. A. N. Mansour, *Surf. Sci. Spectra*, 1994, **3**, 231-238.
14. T. Yamashita and P. Hayes, *Appl. Surf. Sci.*, 2008, **254**, 2441-2449.